International Journal of Science and Research Archive

eISSN: 2582-8185

Cross Ref DOI: 10.30574/ijsra

Journal homepage: https://ijsra.net/

(RESEARCH ARTICLE)

Utilizing Wi-Fi radio frequency energy to power battery-less wearable radios

Abdullah Al Niloy *, Md. Akhtaruzzaman, Romjan Molla, Md Sabbir Hossain, Mohammed Ramzan Ali and Md Sohel Mia

Department of Electrical and Electronic Engineering, Canadian University of Bangladesh (CUB) Dhaka 1212, Bangladesh.

International Journal of Science and Research Archive, 2026, 19(02), 258-265

Publication history: Received on 23 March 2026; revised on 04 May 2026; accepted on 06 May 2026

Article DOI: https://doi.org/10.30574/ijsra.2026.19.2.0962

Abstract

We suggest in this work that batteries can be eliminated by utilizing Wi-Fi communication with surrounding devices including various access points and smartphones to provide power wirelessly to different wearable devices. This would eliminate the need for carrying batteries. A temperature sensor which is wearable that gains energy communication and sends data is something that we are working on developing. We can make this application possible by developing an effective Wi Fi harvesting front-end operating at 2.4 GHz. This front end is used to power an ANT radio platform, and the Wi-Fi source is a smartphone. By studying and analyzing the impact that modulation (OFDM), 72 MHz wide bandwidth, and the bursty feature of 802.11 Wi-Fi signals have on the efficiency, sensitivity, and transmitted power of the RF harvester, we learn how these factors affect the harvester. With a storage capacitor node leakage of 2.5 µW, our prototype can reach a sensitivity of-16.5 dBm. This is achieved through 100% duty cycle Wi-Fi broadcasts without any interference. This translates to a working range of approximately 11.5 centimeters that operates at 2 decibels, and 92 centimeters from a different Wi-Fi access point that operates at 20 decibels and has a 3-decibel antenna on the wearable device.

Keywords: Rf Energy Harvesting System; Battery-Free; Wearable Radio Platform

1. Introduction

The growth of wearable gadgets has been made possible by technological advancements in all of these areas, which have resulted in the devices becoming more compact, and lighter, which is contributing to the development of digital platforms that are smaller, quicker, and more power-efficient. Techniques of microfabrication, often known as MEMS, are paving the way for sensors that are both compact and efficient in terms of power. Increasingly sophisticated methods of production, assembly, and integration are making it possible to create devices that are more compact, lighter, and more cost-effective.

On the other hand, despite all of these developments, the broad acceptance and use of wearable devices have been hampered by limits in the sources of power [1]. The technology behind batteries has not had the opportunity to grow, and as a result, the current method of utilizing batteries supplements additional costs, dimensions, and weight. As a result of their short lifespan and the fact that they need to be recharged and replaced regularly, batteries are a significant disincentive. As the number of wearable gadgets continues to increase and as they strive to obtain wider acceptance and usage models, there is a growing demand for alternative methods that may effectively power these devices [2].

Researchers have looked into solar, thermal, motion, and radio frequency power harvesting over several years to develop battery-free sensing and computation methods [3]. Because we feel that this method offers several benefits for wearable devices, we will be concentrating our efforts in this work on the process of collecting energy from radio frequency sources. Every device must have an antenna to communicate, and in theory, using the same antenna to

* Corresponding author: Abdullah Al Niloy

harvest incoming radio frequency power is possible [4]. Wearable devices are also exceedingly mobile. On the other hand, we are constantly

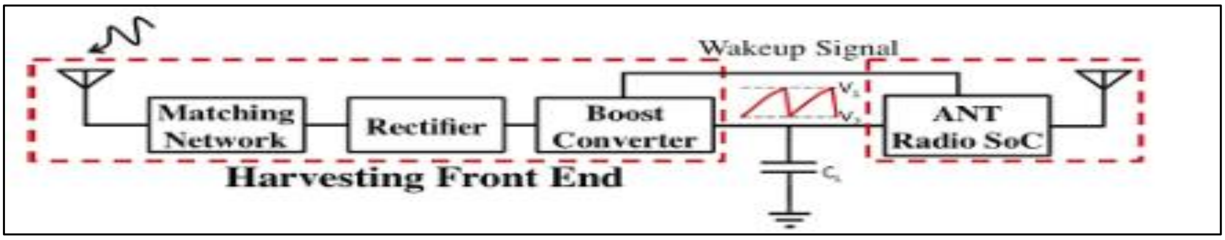

Figure 1 The overall design of the wearable ANT radio platform with Wi-Fi capability

surrounded radio frequency signals, such as those that are transmitted by cellular networks, televisions, and Wi-Fi networks, which have the potential to provide power to small wearable devices [5]. In the following part, we will investigate whether or not the various radio frequency (RF) signals can be utilized as a supplementary power source for wearable devices [6].

2. Architecture of the wearable platform

The platform is designed to be worn while the user is not wearing any batteries. Wi-Fi signals are gathered and used to power all of the components of the wearable platform, including the radio, the temperature sensor, the computer core, and the power management system [7]. In Fig. 1, the structure of the wearable radio platform that is powered by Wi-Fi is displayed [8]. A rectifier (single stage) first transforms the radio frequency (RF) signal to low voltage direct current (DC) [9]. The antenna is responsible for capturing the RF signal and converting it into DC power in a two-step procedure with the antenna. The boost converter is the source of power for the ANT SoC. From a theoretical standpoint, however, given that both ANT and Wi-Fi operate in the 2.4 GHz ISM band, it is possible to multiplex a single antenna between the harvesting and communication front ends, albeit with an additional loss of 0.5 dB through the utilization of a switch that is analogous to [10].

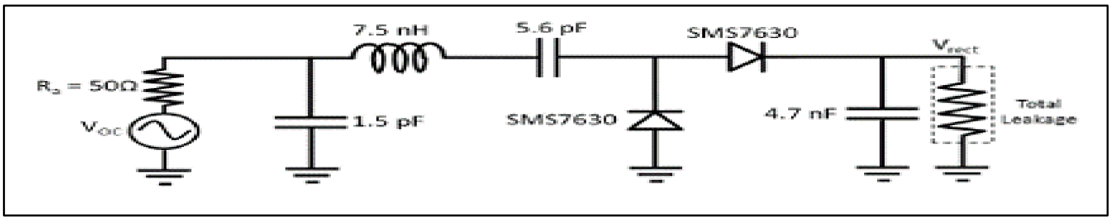

Figure 2 Wi-Fi signals at 2.45 GHz are converted into an output DC voltage via the rectifier's RF front end architecture

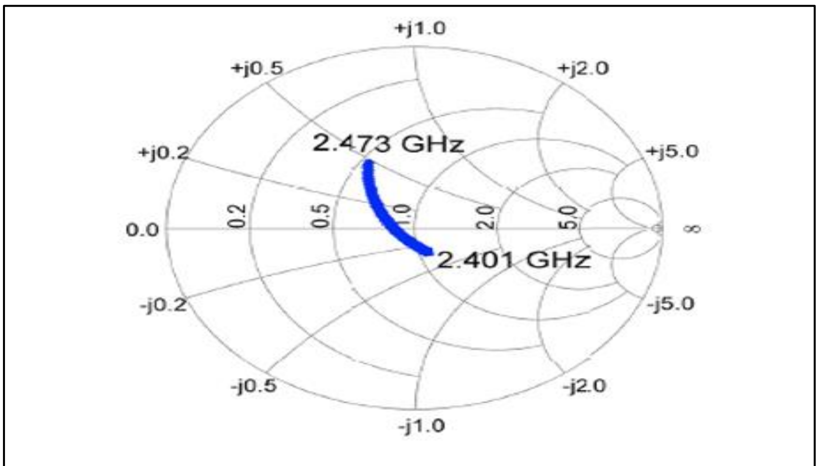

Figure 3 Measured RF energy harvester input impedance for a continuous wave input across the Wi-Fi spectrum at-16 dBm

2.1. Antenna

Because of the rigorous form factor constraints that are imposed on wearable devices, the size of the antenna is restricted, which in turn limits its gain and efficiency [11]. It is for this reason that a directional antenna is not suggested. It was decided to proceed with an inverted F antenna, which offers a satisfactory compromise between antenna gain, size, and output/efficiency. The dimensions of the antenna are 25.7 millimeters by 7.5 millimeters, and it has an efficiency/output coefficient of 80% and a peak gain of 3.3 decibels.

2.2. Matching Network and Rectifier

Both the matching network and the Dickson charge pump (one-stage) rectifier that was utilized in this work are depicted in Fig. 2 [12]. By utilizing low threshold voltage SMS7630 061 Schottky diodes in the rectifier, it is possible to achieve a high level of efficiency in the conversion of radio frequency to direct current [8]. The tuning of the front end was carried out with the assistance of a VNA, and it was modulated to obtain the minimum possible i.p. power sensitivity [13]. A voltage network analyzer (VNA) was used to evaluate the input impedance at a wave input of-16 dBm spanning the range of 2.401-2.473 GHz. The results of this measurement are displayed on a Smith chart in Fig. 3 [14].

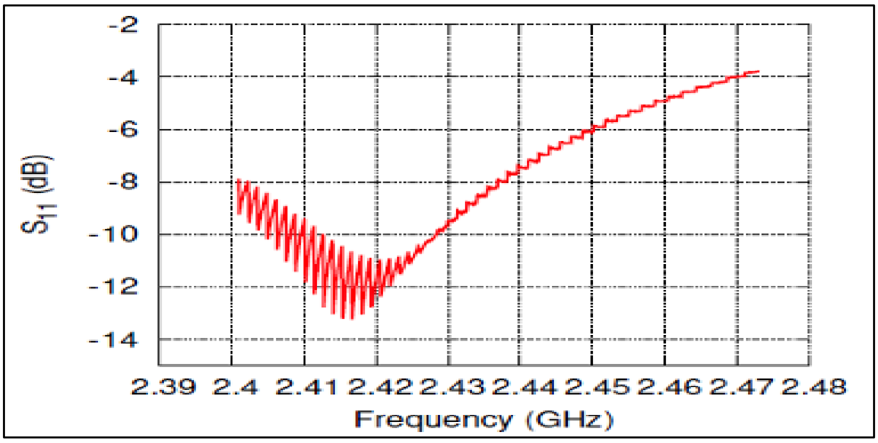

Figure 4 Measured return loss for a continuous wave input of 16 dBm across the Wi-Fi band at the rectifier's input. The boost converter's switching, which is reflected on the RF harvester's input port, is what causes the ripple on the $11

At a particular working frequency, the sensitivity of the rectifier is determined by the leakage power as well as the output voltage that is sought [15]. The leakage of the platform was reduced to the greatest extent possible to achieve high levels of efficiency and sensitivity. In the present study, we have achieved a sensitivity of-16 dBm [16].

An evaluation of the rectifier's sensitivity to a continuous wave input signal was carried out with the help of a voltage network analyzer (VNA), after the matching network was designed. On the other hand, 802.11n Wi-Fi broadcasts make use of OFDM modulation [5]. In the fourth section, we analyze the influence that Wi-Fi signals have on energy harvesting.

2.3. DC-DC Converter

A high-efficiency boost converter is included in the bq25570 [17]. Additionally, the boost converter is equipped with an MPPT mode that is based on voltage (especially after a cold start). Each time the boost is detached for 256 milliseconds, the OCV is recorded and utilized as a reference for the maximum power point tracking (MPPT) algorithm. One example is that the Maximum PowerPoint Tracking (MPPT) can be adjusted to either 80% or 50%, which means that the i.p. of the boost can be regulated to either 80% or 50% of the OCV. On the other hand, because of the non-continuous nature of Wi-Fi packets, wi-fi harvesting cannot be accomplished using this method. If the sampling of the open circuit occurs during a time, then the voltage within the open circuit that is being sampled will be 0. Consequently, the boost converter will pull the input to zero, which will ultimately lead to the collapse of the system. This was done to alleviate the problem that was being experienced. A programmable voltage supervisor is also included on the bq25570 chip. This supervisor was utilized for the system-on-chip (SoC) [18].

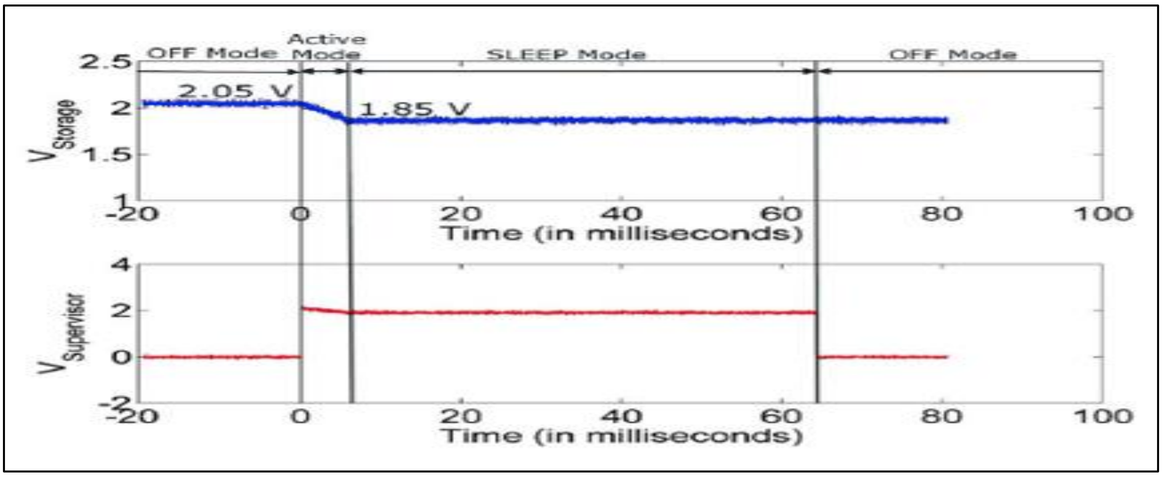

Figure 5 The voltage on the storage capacitor as a function of time and the wake-up signal from the voltage supervisor of the bq25570 chip. The ANT SoC has an annotation for each of its operational modes

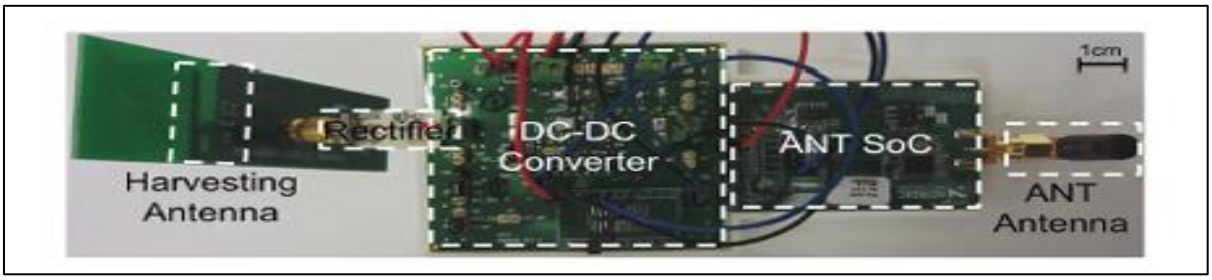

Figure 6 The wearable platform prototype that utilizes readily available components

2.4. ANT Radia SOC

A jump-initiator is started by connecting an external voltage of 1.8V to the storage capacitor. This is done as a compromise. The platform continues to operate continuously while simultaneously sustaining itself on the power that is harvested from the Wi-Fi network. As an alternative, a switchable element might be inserted between the ANT and the shortage capacitor SoC to alleviate the problem that occurs when the ANT is starting up. For instance, it is possible to make use of an LDO that possesses enable functionality that is controlled by the supervisor output.

3. Results of experiments

It is of the utmost importance that we evaluate the harvester while taking into consideration all of these aspects. Furthermore, in contrast to previous research, which concentrated solely on the rectifier, the present study endeavors to assess the effectiveness of the full RF harvesting chain [19].

3.1. RF harvesting with a constant wave source

The harvesting efficiency grows, reaches a maximum, and subsequently decreases with an increase in input power. This phenomenon can be explained by keeping in mind that the rectifier charge pump's RF to DC conversion and impedance matching—which minimizes return loss at the antenna terminal—are what determine the RF to DC efficiency.

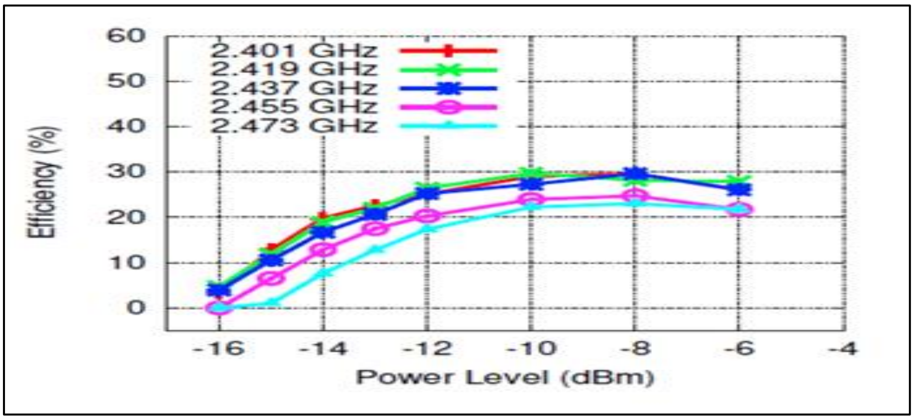

Figure 7 The total RF harvester efficiency as a function of input power and operating frequency for a continuous wave input

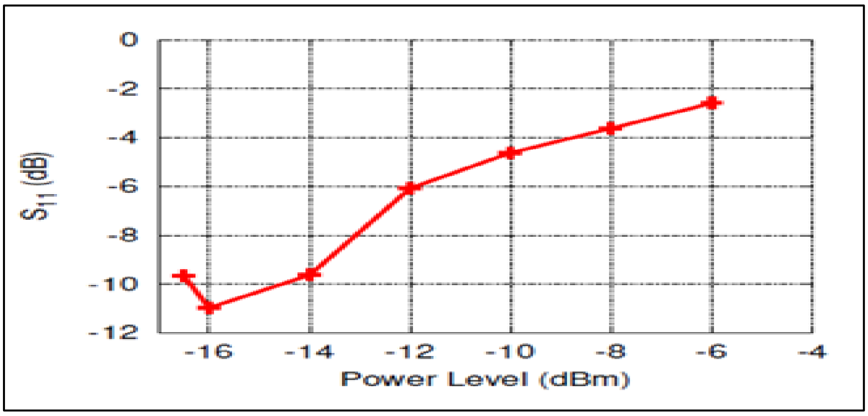

Figure 8 The return loss at the RF front end antenna terminal concerning the input power at 2.412 GHz continuous wave input

The rectifier charge pump efficiency is low at low input power because the voltage levels are almost at the diodes' threshold voltage. Improved rectification in the charge pump's diodes is the result of higher voltage levels at the rectifier charge pump's input as input power is raised [20]. As seen in Fig. 8. This is the result of static impedance matching, which is optimized at the rectifier's sensitivity for a single input power. Additionally, Fig. 7 demonstrates how the harvester's efficiency changes with operating frequency. When compared to 2.455 and 2.473 GHz, the harvester performs better at 2.401, 2.419, and 2.437 GHz.

3.2. Wi-Fi-based RF harvesting as an input

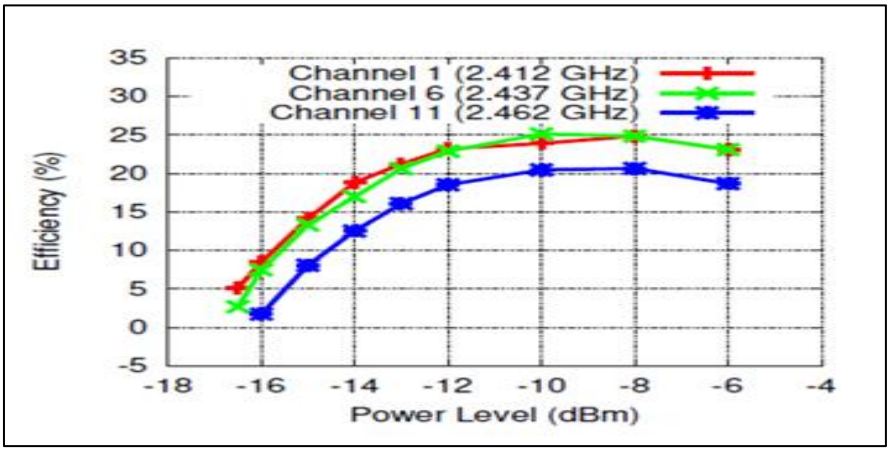

Figure 9 The RF harvester's efficiency for a certain input Wi-Fi signal and its fluctuation based on the Wi-Fi channels

In the following step, we will assess the effectiveness of the harvester by using Wi-Fi signals as input. The rectifier front end was linked to a vector signal generator that was set up to send Wi-Fi packets that were 4091 bytes long, with 64 QAM subcarrier modulation, and with no idle time (i.e., a duty cycle of 100%).

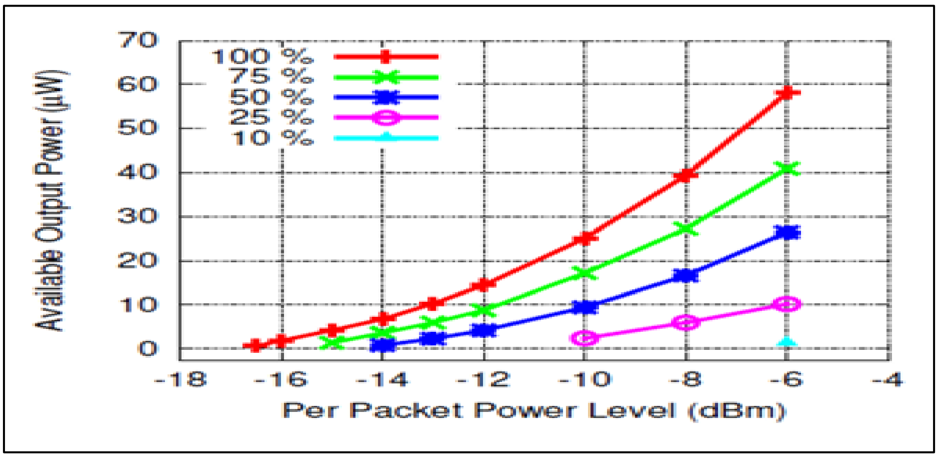

Figure 10 The RF harvester's output power about the duty cycle and input power for 2.4 GHz Wi-Fi transmissions in Channel 6

For each of the three Wi-Fi channels (Channel 1, Channel 6, and Channel 11), the efficiency is depicted as a function of the input power in Figure 9. In contrast to the efficiency for continuous wave input, which is depicted in Fig. 7, but it is higher when the input power is low. The 64 QAM OFDM modulation technique produces peaks and valleys as a consequence of its high peak-to-average power ratio [18]. Because of the exponential nature of diode conduction. This leads to a decrease in efficiency when the input power is high in comparison to when the input is a continuous wave. This is because the gains that are caused by the peaks are greater than the losses that are caused by the valleys, which results in a higher efficiency when the input power is decreased.

3.3. RF energy harvesting based on Wi-Fi duty cycle

Fig. 10 illustrates this, showing the available direct current power at the RF harvesting chain's output. The power of the Wi-Fi transmissions is plotted individually for each packet [21]. This results in a decrease in sensitivity, a reduction in the operational range, and a slowdown in the update rates.

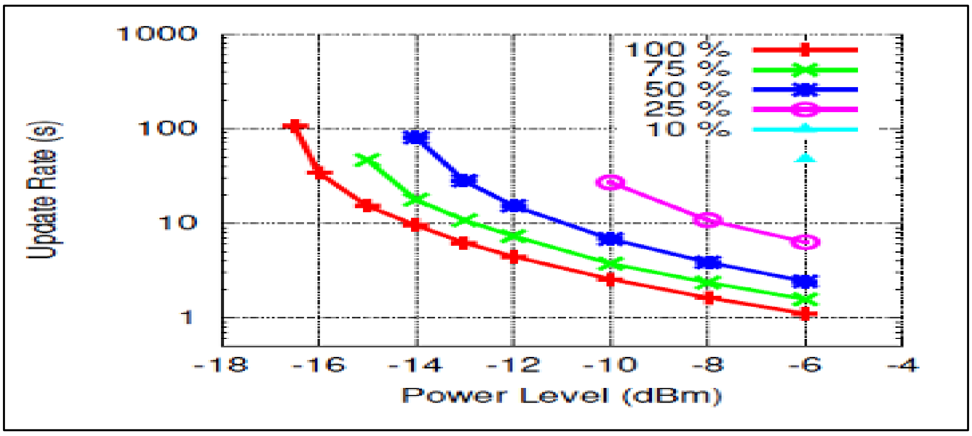

Figure 11 Update rate of ANT radio protocol sensor data transmissions based on Wi-Fi parameters

Taking into consideration that the leakage power of the system remains constant at 2.5 µW, it is possible to intuitively com-prehend this phenomenon. However, when the duty cycle is reduced, the average power decreases in linear form, resulting in a decrease in the amount of power that is accessible at the output.

3.4. Rate of sensor update based on the features of the Wi-Fi network

A representation of the update rate of the temperature sensor is shown in Fig. 11. The wearable platform updates at a rate of a few seconds. Nevertheless, the temperature update rate drops to one reading every 100 seconds, which is a result of either decreased input power or decreased duty cycle. It is necessary to collect a data point every couple of minutes for ordinary sensor applications; hence, Wi-Fi harvesting is an appropriate solution for these conditions.

3.5. Utilization of a wearable platform in conjunction with a Smartphone

Last but not least, we analyze the performance of the entire wearable platform. On the other hand, as was said earlier, the transmit power of smartphones is decreasing. To determine the average, transmit power of Wi-Fi broadcasts per packet, we carried out experiments in both an anechoic room and a more traditional laboratory environment. After de-embedding the antenna gains and applying the Friis equation, we were able to find out through experimentation that the average transmits power of ordinary smartphones, taking into account the losses caused by the antenna and the enclosure, is approximately 2 dBm per packet.

In the following step, we will maximize the duty cycle by setting up the smartphone to function as a Wi-Fi hotspot. In the course of our trials, we were able to obtain a maximum operational distance of 11.5 centimeters between the smartphone that was functioning as a Wi-Fi hotspot and the wearable platform that was created to be powered by Wi-Fi.

4. Conclusion

We have developed the first Wi-Fi-powered radio platform as a result of this study. We not only presented the design and analysis of the Wi-Fi harvesting chain, but we also looked at how the harvester's performance is affected by the duty cycle, OFDM modulation, and broadband nature of Wi-Fi transmissions. With a target output voltage of 2.05 V and a platform leakage of 2.5 µW at the output, our prototype can reach a sensitivity of-16.5 dBm. This is achieved through 100% duty cycle Wi-Fi transmissions. The Wi-Fi-powered radio platform that was built is capable of functioning at a distance of up to 11.5 centimeters from a Wi-Fi transmitter that operates at 2 decibels (on a standard smartphone).

Compliance with ethical standards

Disclosure of conflict of interest

No conflict of interest to be disclosed.

References

[1] A. Ometov, V. Shubina, L. Klus, J. Skibi´nska, S. Saafi, P. Pascacio, L. Flueratoru, D. Q. Gaibor, N. Chukhno, O. Chukhno et al., "A survey on wearable technology: History, state-of-the-art and current challenges," Computer Networks, vol. 193, p. 108074, 2021.

[2] L. M. Correia, D. Zeller, O. Blume, D. Ferling, Y. Jading, I. G´odor, G. Auer, and L. Van Der Perre, "Challenges and enabling technolo gies for energy aware mobile radio networks," IEEE Communications Magazine, vol. 48, no. 11, pp. 66–72, 2010.

[3] X. Zhou, S. Cheng, X. Wu, and X. Rao, "Influence of photovoltaic power plants based on vsg technology on low frequency oscillation of multi-machine power systems," IEEE Transactions on Power Delivery, vol. 37, no. 6, pp. 5376–5384, 2022.

[4] Z. Lai, J. Xu, C. R. Bowen, and S. Zhou, "Self-powered and self-sensing devices based on human motion," Joule, vol. 6, no. 7, pp. 1501–1565, 2022.

[5] M. Wagih, L. Balocchi, F. Benassi, N. B. Carvalho, J.-C. Chiao, R. Correia, A. Costanzo, Y. Cui, D. Georgiadou, C. Gouveia et al., "Microwave-enabled wearables: Underpinning technologies, integration platforms, and next-generation roadmap," IEEE Journal of Microwaves, vol. 3, no. 1, pp. 193–226, 2022. [6] P. Tielens and D. Van Hertem, "The relevance of inertia in power systems," Renewable and sustainable energy reviews, vol. 55, pp. 999 1009, 2016.

[6] M. A. Al Mamun and M. R. Yuce, "Sensors and systems for wearable environmental monitoring toward iot-enabled applications: A review," IEEE Sensors Journal, vol. 19, no. 18, pp. 7771–7788, 2019.

[7] E. Nu˜no, P. Maule, A. Hahmann, N. Cutululis, P. Sørensen, and I. Karagali, “Simulation of transcontinental wind and solar pv generation time series,” Renewable energy, vol. 118, pp. 425–436, 2018.

[8] A. C. C. Chun, H. Ramiah, and S. Mekhilef, “Wide power dynamic range cmos rf-dc rectifier for rf energy harvesting system: A review,” IEEE Access, vol. 10, pp. 23948–23963, 2022.

[9] X. Tang, “Privacy-preserving sensing and wireless communications for iot-enabled smart environments,” Ph.D. dissertation, Case Western Reserve University, 2020.

[10] T. Sztyler, H. Stuckenschmidt, and W. Petrich, “Position-aware activity recognition with wearable devices,” Pervasive and mobile computing, vol. 38, pp. 281–295, 2017.

[11] T. Schumacher, P. Fath, S. Schmickl, T. Faseth, P. Hetterle, R. Weigel, and H. Pretl, “A design-for-sensitivity strategy for charge-pump-based receivers,” in 2020 Austrochip Workshop on Microelectronics (Aus trochip). IEEE, 2020, pp. 13–20.

[12] A. Mohan and S. Mondal, “A multi-band impedance matching strategy using lumped resonant circuits,” Circuits, Systems, and Signal Process ing, vol. 42, no. 3, pp. 1369–1388, 2023.

[13] A. J¨ager-Waldau et al., “Pv status report 2019,” Publications Office of the European Union: Luxembourg, pp. 7–94, 2019.

[14] A. C. Sun, C. Yao, A. Venkatesh, and D. A. Hall, “An efficient power harvesting mobile phone-based electrochemical biosensor for point-of care health monitoring,” Sensors and Actuators B: chemical, vol. 235, pp. 126–135, 2016.

[15] Y. Guan, Y. Wang, W. Wang, and D. Xu, “Analysis and design of a high-frequency dc/dc converter based on a resonant rectifier,” IEEE Transactions on Industrial Electronics, vol. 64, no. 11, pp. 8492–8503, 2017.

[16] D. Karunatilaka, F. Zafar, V. Kalavally, and R. Parthiban, “Led based indoor visible light communications: State of the art,” IEEE communi cations surveys & tutorials, vol. 17, no. 3, pp. 1649–1678, 2015.

[17] R. Niwareeba, “Peak-to-average power ratio reduction in optical-ofdm systems using lexicographical permutations,” Ph.D. dissertation, Faculty of Engineering and Built Environment, University of the ..., 2023.

[18] A. Verma and S. Singhal, “Solar pv performance parameter and recom mendation for optimization of performance in large scale grid connected solar pv plant—case study,” J. Energy Power Sources, vol. 2, no. 1, pp. 40–53, 2015.

[19] K. Miwatashi, T. Hirakawa, N. Shinohara, and T. Mitani, “Development of high-power charge pump rectifier for microwave wireless power transmission,” IEEE Journal of Microwaves, vol. 2, no. 4, pp. 711–719, 2022.

[20] A. Dziedzic, V. Sathya, M. I. Rochman, M. Ghosh, and S. Krishnan, “Machine learning enabled spectrum sharing in dense lte-u/wi-fi coex istence scenarios,” IEEE Open Journal of Vehicular Technology, vol. 1, pp. 173–189, 2020.